# Experimental evaluation of hydroacoustic instruments for ROV navigation along aquaculture net pens

Per Rundtop and Kevin Frank, SINTEF Fisheries and Aquaculture, 7465 Trondheim, Norway

## Introduction

Holes in the net constitute a challenge with respect to fish escapes in modern aquaculture using gravity net pens. More than two thirds of the registered escape incidents in Norwegian salmon farming are related to holes in the net (Jensen et al. 2010). One important measure in Norway to reduce the risk of escapees is the mandatory net inspection after all kind of operations involving the net and weighting system. This demand ensures that holes caused by such operations are discovered and consequently repaired as early as possible, minimizing the period with non-intact net structure. For this purpose, but also for regular net cleaning operations (removal of biofouling organisms from the net), Remotely Operated Vehicles (ROVs) have been proven to be a safe, robust and in many cases cost-effective alternative to divers.

To date, ROVs are mainly used inside the net pen, as ROV operation outside the net pen is complex due to the surrounding mooring system and lead to increased risk of tether entanglement. Inside the cage the vehicle is usually moved manually in horizontal or vertical transects close to the net. The ROV pilot bases the steering usually on information from a forward looking camera, a depth sensor and a compass. This type of instrumentation gives no well-defined position-coordinates for the ROV relatively to the net pen. Thus the precision of the desired path along the net pen is dependent on operator experience and environmental conditions, which include turbidity, light, currents and wave state. It is currently not possible to reliably document the inspected net pen area using this type of ROV operation. Consequently, full coverage (100% of submerged net area) of net inspections cannot be ensured. To enable true control of the path and allowing reliable documentation of net coverage, a new navigation system for ROVs is required. It is necessary that this system provides net pen relative position data and not absolute positions. This is because gravity net pens deform by current induced drag forces (Lader et al. 2008), e.g. up to 20% in reduced net pen volume when they are subjected to a current

velocity of 0.5 m/s has been reported (Klebert et al. 2015). Meaning that the shape of the inspected net cannot be predetermined. Hence, navigation for net operations has always to be done relatively to a dynamic and unknown net pen shape. Combining such navigation system with a guidance and motion control system will enable net pen tracking using autonomous underwater vehicles (AUV).

There are several underwater navigation systems available, which are usually applied in open water or in range to steady solid formations. They are commonly categorized as (Paull et. al 2014):
1) Acoustic transponders and modems which provide absolute position information with bound navigation errors but have a low output frequency
2) Dead reckoning systems which provide robust and high frequency navigation data but accumulate errors in position over time
3) Systems based on the geophysical navigation methods, which are based on detection and identification of external environmental features as references for navigation

Modern underwater navigation often integrates sensors from different categories into one system to overcome their individual weakness and fully utilize their strengths. In consequence were the following two state-of-the-art hydroacoustic sensor systems from two different categories selected for the presented work:
1) an Ultra Short Base Line (USBL) system
2) a Doppler Velocity Log (DVL) system

We examined the ability of both systems to enable navigation inside a net pen, with a perspective to eventual multisensory fusion. This could be based on e.g. a Kalman filter (Kalman, 1960), consisting of a numerical model of the vehicle getting input from the individual navigation systems.

The hydroacoustic USBL principle is well-known and used routinely in a number of applications. USBL systems are composed of a transceiver mounted at a reference position (e.g. at a surface vessel) and a transponder on an underwater vehicle. The position of the underwater vehicles relative to the surface vessel is calculated from the transmission distance and bearing (Vickery, 1998).

DVL systems are also popular as navigational tools for ROV's, autonomous underwater vehicles, and human-occupied vehicles. These systems, commonly based on multiple hydroacoustic beams pointing downwards to the seabed, analyses the Doppler shift in bins reflected by the seafloor, to determine the vehicle’s velocity and altitude over ground (Rudolph and Wilson, 2012). By mathematical integration of the vehicle velocity the travelled distance and relative positions to the starting point can be calculated. Thus, DVL systems can perform as a fundamental component for dead reckoning underwater navigation systems.

The combination of USBL and DVL systems has been proven to be effective for navigation of underwater vehicles in open water. However, navigation within aquaculture net pens presents entirely different conditions and challenges. In this application, DVL system would function as a net relative sensor to provide net pen relative velocity and positioning data, which is required when pen shape can not be predicted. This requires the DVL system to be able to detect the net with its significant lower target strength (Mooney et al., 2004) compared to the seabed.

A further potential constraint is the dense biomass of fish contained in aquaculture net pens. In Norway, up to 200 000 fishes amounting to a biomass of 800 tons can be contained in a single net pen. This can result in limitations for the use of hydroacoustic instrumentation, due to scattering from the air-filled swim bladders of fish (Foote, 1980). The DVL and USBL systems are expected to be affected differently by this phenomenon. A DVL faces the net and the distance between the DVL system and the net is expected to only be a few meters. The USBL system will provide reliable absolute positions in the whole net pen volume. Therefore, the probability for biomass to interfere with the USBL system’s hydroacustic signal path is expected to be higher than for the DVL system.

Based on these application specific operational uncertainties, this work focused on the following objectives using full-scale experimental investigations:
i) Identify the following key performance properties when operating an USBL system within a net pen volume with industrial scale biomass:
a) ROV position coverage of the net pen volume

b) Updating rates on position coordinates in the net pen volume

c) Precision and noise levels for the reported position

ii) Identify the ability of the DVL system to:

a) Log and track on the net pen

b) Measure net relative distance and orientation

c) Measure net relative velocity and identify dead reckoning capabilities

## Materials and methods

### Notation

Position coordinates and vehicle velocities are given for further discussion of the experiments and results in the standard notations for a vehicle with 6 degrees of freedom (DOF) in Table 1 and set by (SNAME, 1950).

It is convenient to define two reference frames (Fossen, 2011) for such navigation systems. The positions measured by the USBL system are expressed in a frame which is earth-fixed and denoted as *North-East-Down* (*NED*). The second frame, the *BODY* reference frame, is a moving coordinate system fixed to the vehicle, where the x-axis points from aft to fore, y-axis directed from port to starboard and z-axis pointing from top to bottom. The velocity measured by the DVL system on the vertical net pen wall is expressed in this frame. The position and orientation of the ROV towards the net are defined as in Table 2.

### ROV and surface vessel

For the experiments an Argus Mariner (Fig. 1) ROV from Argus Remote Systems AS was used. This type of ROV falls into the "observer" or "small working ROV" class that is used for commercial aquaculture net and mooring inspection tasks. During the trials, the ROV was operated by a professional ROV-pilot by the aid of an onboard HD video camera. The mass of the ROV is approximately 600 kg, with dimensions for length, width and height of 1.6 m, 1.1 m and 0.9 m, respectively. The ROV was equipped with 2 vertical and 4 horizontal thrusters, and actuated in 4 degrees of freedom (surge, sway, heave and yaw). The ROV was operated from an aquaculture service vessel, moored to the floating collar of a net cage.

**Experimental conditions**

The experiments were performed at a commercial salmon farm located off the coast of mid-Norway. A circular gravity net pen with plastic floating collar with 50 m diameter was used. The net pen had vertical net walls to a depth of 15 m and a conical shaped bottom, with the deepest point at 25 m depth. The net pen was a nylon net with a mesh size (bar length) of 15 mm and a twine diameter of 2-3 mm. The net pen contained a biomass of 302 tons (*Salmo salar*) with an average fish weight of 1.76 kg. The weather during the experiments was calm, with almost no waves at the site. The site is not known for halocline occurrences. There was no feeding ongoing during the trials. Observation gave a rather homogenous and low degree of biofouling for the whole observable net pen.

**USBL system survey**

A Scout Plus USBL system from Sonardyne International Ltd. was used in the experiments. The system is composed of an 8024 transceiver and a WSM6 transponder type 8271. This system is designed for a slant range of 500 m and utilizes 35-55 kHz as operational frequency band. The accuracy is given as ± 2.75 % of the slant range.

The transceiver was deployed at approximately 2 m water depth on a pole fixed to the surface vessel (draft 1 m, beam 8 m), at port side (boat moored on the starboard side, see Fig. 2). Sonardyne's standard software was used for data logging. The sample interval was set to the minimum possible value of 1 second. The Sonardyne system can measure changes in the transceiver's roll, pitch and yaw angles (Sonardyne, 2007) and includes this information in the data processing. However, during the experiments, only the yaw sensor was operational so that changes in roll and pitch could not be compensated. However, the boat was a heavy catamaran and the sea state was very calm during the period for the experiments. Hence were there only minimal movements of the transceiver which are not expected to have a significant impact of the on the results.

During the experiments, two different methods were used for deployment of the transponder. It was either placed onto the ROV or attached to a rope for manual positioning. The experiments with manual positioning of the transponder were done

along the floating collar at pre-defined net pen circle positions (Fig. 2). The net pen circle position was obtained by counting the number of brackets of the floating collar each representing 6 degrees. The transponder was attached to a guide rope attached with a metal weight, and was placed at the end of a rope and the transponder depth was adjusted manually using markers on the rope. The rope was lowered on the outside the floating collar (approximately 1 m horizontal distance to the net).

We conducted 5 separate experiments (U1-U5) with the USBL system, with both manual positioning of the transponder and positioning with aid of the ROV. The five testing conditions are described as follows:

**U1) Performance in open water:** The ROV carrying the transponder was placed at the seabed in 14 m depth in a slant range of approximately 155 m from the transceiver with only open water between them. This trial provides data for estimating the noise in the position signal of the USBL system without biomass or other obstacles in the transmitting path. Data was logged for 3 minutes, giving a possible maximum of 180 sampled positions.

**U2) Biomass interaction**: To quantify the impact of the biomass on the transmission of the hydroacoustic signal, manual positioning of the transponder was done at the net pen circumference. Data was collected at three depths (2, 8, 15 m), and 10 net pen circle positions in the range 0-180° (Fig. 2). Each position was maintained until 3 minutes of data were obtained.

**U3) Net pen interaction:** The net pen impact on the USBL signal was investigated by positioning the transponder, placed on the ROV in 5 m depth close to net, at net pen circle positions of 0° and 180°, both inside and outside the net pen. At all four positions data were logged for 3 minutes.

**U4) Increased distance, amount of biomass and net:** To investigate the performance with even higher biomass in transmitting path, was the ROV carrying the transponder placed in approximately 215 m distance from the transceiver and in 12 m depth behind a row of 3 commercially stocked net pens. Data was logged for 3 minutes. In proportion to the increased transmission length, also the biomass and the amount of netting in the communication path were approximately tripled compared to the 180° outside net pen position in U3.

**U5) Net inspection pattern:** The ROV moved in a repeated upward/sideways/downward/sideways pattern along half of the cylindrical net pen wall (0°-180°). The depth range of movement was 0-15 m, while the sideways movement was approximately 4 m. Subsequently approximately a 1/3 of the conical net pen bottom was inspected as well. This part of the pattern was done by moving radially, along the wall of the cone between the bottom tip and different net pen circle positions at the sinker tube. As this requires moving the ROV continuously on all three axes of the NED frame, the resulting pattern along the net pen bottom is less well defined than the path along the net pen wall, where movement only sideways and in depth are required.

The USBL positions in the NED-frame were obtained from the vendor software and, if not specified, presented after outlier removal. For the experiments U1-U4, north, east o r

d After outlier removal the position update intervals were calculated. Update intervals a are given for experiments U1-U4 as average, for U2-U3 also as minimum and m aximum. For experiment U5 the update interval for each sample was calculated as the elapsed time since the previous sample. In general, the update interval provides a n indication of transmission challenges and noise levels, and has to be seen in o ontext with the requirements of an integrated navigation system. Also the standard d eviation for position coordinates ($\sigma_{PC}$) in pre-defined periods (3 min) was calculated f or experiments U1-U4. $\sigma_{PC}$ was here used to evaluate noise levels and consistency o f the position measurements and given for the north, east, down coordinates s eparately.

e

**D VL system surveys**

t A Teledyne Workhorse Navigator DVL system with an operation frequency of 1200 k Hz was used in the trials. The DVL system was mounted to the frontal side of the ROV pointing forward (Fig. 3). As the DVL system was fixed to the vehicle, the v elocity and position coordinates from this instrument are given in *BODY* reference f rame.

t

h

The DVL system was powered from the ROV power supply and connected to a computer on the aquaculture service vessel via the ROVs RS232 interface. Data was logged using the vendor's software during the experiments. Only a few DVL system configuration parameters were set (Table 3); all other parameters were according to default settings. These settings were picked based on preliminary tests and discussions with the DVL system producer.

Three experiments with focus on the DVL were performed. The experiments were conducted while the DVL faced the vertical net pen wall.

**D1) Net-ROV-distance:** The DVL system's ability to measure the distance *d* between ROV and net inside the pen was tested. For this experiment the ROV remained stationary several seconds in different distances to the net wall, facing it as orthogonally as possible.

**D2) Net relative yaw angle:** The ability to measure net relative yaw angle $\alpha$ was tested by pivoting the ROV from left to right, while keeping its distance to the net and depth as consistent as possible.

**D3) Velocity and dead reckoning:** The ROV was steered in a rectangle pattern facing the net. The start and end point was located in the upper left corner of the rectangle, and ROV was moved in the following pattern: downward, sideways right, upward, sideways left. The ROV was moved twice in this pattern. The rectangle was predefined by the vertical and horizontal rope net structure integrated in the net pen. Based on data from the net pen manufacturer, the rectangle defined by the rope structure had a size of 7.5 x 5 m (horizontal x vertical). The ROV was driven manually by aid of its camera. Start and end point were observed as equal for both runs. The ROV pilot tried his best to keep the net relative angle close to zero and the distance to the net constant while moving along the net. Observation from the camera video stream leads to the rough estimation of a repetition-accuracy for the rectangular corners of approximately 0.5 – 1 m.

Net relative distance is provided by the instrument software, as in the usual applications vehicle altitude is calculated. The system also calculates the altitudes $b_1$, $b_2$, $b_3$, $b_4$ based on the distance data from the individual beams (B1, B2, B3, B4 (Fig. 3)). With the estimate that the net is a vertical plane and the ROV has no pitch and

roll angle, these altitudes in combination with the known DVL beam angle of 60° can b
e $\alpha = \tan^{-1}(BC / AB)$ 1)

With BC and AB defined as:

$AB = a_1 / \tan(60°) + a_2 / \tan(60°)$ 2)

$BC = a_2 - a_1$ 3)

Unless specified, the data presented are non-filtered data as provided by the vendor software. Video material, which was recorded from the ROV camera, was used to obtain a visual impression of the fish density between the net and ROV during the analysis.

## Results

### USBL

U1 – Performance in open water

The NED position timeseries is plotted in Fig. 5. The *standard deviation for position coordinates ($\sigma_{PC}$)* was 1.1 m, 0.7 m and 0.3 m for the north, east and down coordinates, respectively. The average update interval was nearly 1 s, as from the 180 raw data samples only one outlier was removed. The results are as expected and within the specified instruments accuracy.

U2 – Biomass interaction

USBL positions from U2 can be plotted against expected positions based on an assumed circular shape of the floating collar and deployment depth of the transponder (Fig. 6). Except for two of the deployed transponder positions (net pen circle position 162° and 180°, both at 2m depth) was the USBL system able to obtain its position.

The average update interval (Fig. 7) at net pen circle positions between 0° and 72° is close to 1 second, which was equal to the configured sample interval for the USBL system, meaning that most of the samples are received and without outlier removal. For these positions also similar update intervals were obtained at different depths. For net pen circle positions above 90° longer average update intervals of 2 - 4.5 s

were found. These also vary with transponder deployment depth. At 2 m depth and at the net pen circle positions 162° and 180° no samples were recorded during the 3 minute sampling period.

In the net pen circle position range 0-54° (all depths) are all $\sigma_{PC}$ smaller than 0.5 m (Fig. 8). However, at larger net pen circle positions $\sigma_{PC}$ were clearly larger, which means higher levels of noise compared to the smaller net pen circle positions. The $\sigma_{PC}$ for the north axis was generally the largest. The $\sigma_{PC}$ for the down axis, up to 108° for depth 2 m and up to 160° for depth 8 m and 15 m, was greater than for the east component. However this is changing towards highest net pen circle positions where the $\sigma_{PC}$ for the east axis is larger.

U3 – Net pen interaction

The position time series for all four cases, inside and outside the net at 0° and 180° net pen circle position, showed different levels of noise (Fig. 9 A). Both time series from the 0° net pen circle position were much smoother than the other two. This is also documented by higher $\sigma_{PC}$ for the 180° net pen circle position, where the outside position had by far the largest $\sigma_{PC}$ in the trial (Fig. 9 C).

The average update interval inside and outside the net at 0° net pen circle positions are 1.02 s. Thus 176 samples of the 180 send from the transponder were received. For the net pen circle positions of 180°, the average update intervals were 1.05 s and 2.52 s for inside and outside net pen, respectively. This long update interval is based on 71 samples, which resulted from the removal of 22 outliers from the 93 received raw data samples.

U4 - Increased distance, biomass and net

The average update interval for the U4 experiment is 7.5 s as 64 samples were acquired, from which 40 are outliers. The $\sigma_{PC}$ of this experiment which had the longest slant range (215 m) of all experiments done with the USBL system is 2.04 m, 2.60 m and 0.49 m for the north, east and down position component, respectively. The experiment indicates that the USBL system is able to obtain the position with longer distance and more biomass in the transmission path. However, the samples are received with large noise levels and long update intervals.

U5 - Net inspection pattern

For 95% of the received positions in depths below 4 m the update interval was 1 s (Fig. 10) and did not exceed 12 s. However, for depths above 4 m the position was not updated for longer periods on several occasions. The maximal update interval obtained was 83 s. This indicates that the USBL system is well working in the net pen environment for depths below 4 m, but having trouble obtaining its position in shallow water.

**DVL**

D1 – Net distance

Results from a preliminary experiment (not further discussed), in which a piece of netting was placed in predefined distances to the DVL system, indicated that the system is capable of calculating the correct net relative distance. However, the minimum distance the DVL system is capable of measuring at the given settings is approximately 1.5 m (Fig. 11, marker b), and produces low noise distance measurements up to 3.5 m (Fig. 11, marker d). The signal quality is dependent on free acoustical beams paths. Hence, the ability to obtain reliable measurements diminishes when fish swim between the DVL system and the net (Fig. 11, marker c). In this trial, the maximum distance measured by the DVL system was 7 m; however, at this distance it was difficult to obtain an obstacle free path.

D2 – Net relative yaw position

The net relative yaw angle calculated from the individual beam distances for experiment D2 is shown in Fig. 13. The distance between ROV and net was approximately 4 m and occasionally fish was present between the DVL and the net.

D3 – Net relative velocity and dead reckoning

The measured data from the DVL system is presented in two time series as the ROV velocity in sway (v) and heave (w), representing displacement along the net sideways and in depth, respectively (Fig. 14 A). For this specific experiment, an update interval of 0.2 s for 90% of the measurements was achieved (Fig. 14 D). However, for some short periods (<2.5 s) no velocities were measured by the DVL

system. This is most likely caused by fish within the vicinity of one or more of the four beams, which was also observed during the experiment.
Position components with respect to the net pen and the starting point could be calculated by mathematical integration of these velocity components with known update intervals (Fig. 14 B and Fig. 14 C).

During the D3 experiment also USBL data were acquired. The data for the depth dimension from both system data can hence be compared. This is based on the assumption that the surge velocity is close to zero as well as roll and pitch angles, as the ROV has passive roll and pitch stability especially at the given calm sea state. Assuming a vertical net pen, only the yaw angle needs to be accounted for when transforming the velocity from *BODY* to *NED*. From eq. 4 it could be seen that a yaw angle different from zero will affect u and v, while $w_{BODY}$ and $w_{NED}$ has 1:1 relationship regardless of yaw angle.

$$[u, v, w]^T_{NED} = R_z * [u, v, w]^T_{BODY} \quad (4)$$

Where the z-axis rotation matrix R, are defined as in (Fossen, 2011):

$$\square\square\square = \cos\square(\square) - \sin\square(\square) 0 \sin\square(\square) \cos\square(\square) 0 0 0 1 \quad (5)$$

In Fig. 15 A are the time series of the vehicles depth obtained directly from USBL system and calculated via dead reckoning from DVL data plotted. The position obtained from the DVL system is smoother and with smaller sample interval compared to the more noisy USBL position. The results also indicate that the difference between DVL and USBL in heave position is increasing in a very consistent pattern as the ROV is traveling further away from the starting point (Fig. 15 B).

## Discussion

Experiment U1 in open water and with fixed vehicle position provides a long range reference for the USBL system performance. The obtained standard deviation for position coordinates ($\sigma_{PC}$) for the three coordinates north, east and down are in the range 0.3-1.1m. The equivalent figures for standard deviation in a spherical coordinate system in which the USBL actually works are 0.4m (slant range), 0.4°

(azimuth) and 0.1° (elevation). This is within the specified instruments accuracy of 4.1 m for a slant range of 150 m. As expected, the system is capable of determining a transmitter position for all samples in the 3 min period, even though one sample falls outside the outlier criterion.

The biomass and underwater structures of the net pen which are placed in the USBL system pathways are expected to dampen and scatter the transmitted hydroacoustic signal. Hence, it was not certain how the system would function under these conditions. At fixed deployment of the USBL transponder at several depths and locations under the floating collar, the horizontal position and the adjusted depth could be reproduced to a certain extent (U2). Hence it could be demonstrated that the USBL system is principally well-functioning in the net pen environment. It is obvious that changes in the experimental conditions have an impact on this statement. The USBL system functionality is expected to at least depend on the deployment method of transmitter and transceiver, the type of used USBL system and used operation frequency, amount of biomass and its distribution.

In the U2 experiment increases the update interval between a net pen circle position of 54° and 72°. This is partly caused by less samples received and partly caused by more samples not fulfilling the outlier criterion. Also increases the standard deviation for position coordinates around this net pen circle position. For the larger net pen circle positions a $\sigma_{PC}$ up to 2.25 m is obtained. Compared to the results from U1 these $\sigma_{PC}$ are increased. This can be explained by the USBL transmitting path is not passing through the net pen at a net pen circle position smaller than approximately 70° (Fig. 2). For the data collected at higher net pen circle position signal scattering and damping by fish swim bladders or the net pen can reduce the acoustic signal intensity and signal-to-noise ratio and result in reduced accuracy. This hypothesis is supported by the signal strength and signal-to-noise ratios (both not shown) reported by the instrument vendor software, as both numbers step down between a net pen circle position of 54° and 72°.

In general the obtained position noise levels are similar, i.e. standard deviations for position coordinates ($\sigma_{PC}$), and the resulted update intervals are in an acceptable range with respect to a final application. Especially when keeping in mind that a

navigation system for net inspection might also include data from other instruments as depth sensor and possibly a DVL system.

The deviation in the horizontal position between the reference system and the USBL north/east coordinates, as indicated in Fig. 6, is very consistent for all three depths. Hence, the deviation is expected to be a consequence of inaccurately estimated reference position. This might be as the collars of gravity net pens are known not to be perfect circles, as forces from mooring bridles and currents shape them oval.

In experiment U3, different $\sigma_{PC}$ were found for the different positions (Fig. 9 C). This is, as described before, likely a result from different interactions of the hydroacoustic signal e.g. crossing the net pen and being scattered by fish swim bladders. In accordance the position signals are less noisy and $\sigma_{PC}$ is smaller at net pen positions 0° than at 180°. Whether this difference is caused by impact from the net pen or biomass is less clear. For the net pen circle position of 180° a difference in $\sigma_{PC}$ is found for outside and inside the net, while at the net pen circle position at 0° this difference is negligible. However, the signal strength of the USBL system (not shown) is similar for both net pen circular positions at 0°. This indicates that the net has a rather low impact on the signal strength. In that regard is it more plausible to explain the differences between inside and outside the net at the 180° net pen position with changes in the biomass distribution. More than 1 hour passed between these two tests and the distribution of fish in the net pen may have changed, resulting in less preferable condition for hydroacoustic transmitting through the net pen.

The USBL results are presented and discussed in position components north, east and down as needed for the targeted application of net inspection, as already mentioned is the USBL system measuring a distance and two angles. In U3 standard deviation of all coordinates at the 0° net pen circle positions are smaller compared to experiment U1 with ROV fixed positioned at the seabed. However, the relative slant range error and the angle errors of the USBL systems spherical system are quite comparable with the results from U1.

The noise in the position signal is expected to be strongly dependent on the biomass in the transmission pathway in the net pen. However, the net pen in this experiment

had approximately 40% of the biomass a net pen of its size usually contains at the final production stage. In U4 a higher biomass was placed in the transmitting pathway, which was in amount comparable to the 800 tons expected in a net pen upon harvesting. Beside the increased biomass and huge distance the USBL system shows an acceptable performance. Hence it appears that an USBL system might function around a net pen until the end of the whole production cycle when the highest biomass is reached. Nevertheless, it is necessary to point out that even though the biomass in the transmitting path was comparable, the density of fish was much lower than at the final stage of production. Hence further testing is required to test the generality of our results.

The USBL system functionality in the net pen was demonstrated in experiment U2. The obtained position noise and update intervals from U2 were expected to be representative for the given case. Hence data from U5 with the ROV as transponder carrier, i.e. less determined positions, are expected to be reliable in the tolerances given from U2. The results from U5 confirm that the USBL system is capable to document an inspection path. While looking at Fig. 10 A and Fig. 10 B it is obvious that simple visualization of the path is possible.

The experiment with the DVL system mounted to the ROV fronting the net in variable distance, confirms unpublished data from preliminary experiments (Frank, unpubl, 2013). The DVL system detects the net as the "bottom" with the applied settings. Results from experiment D1 show how the use of a DVL system allows gathering objective data on net relative distance. These data can substitute the operator's subjective distance estimation based on video and allow visual or machine vision net inspection at constant range. Finally, this leads in combination with the USBL to the ability to determine the net shape and ensure proper coverage.

The results of experiment D2 confirm that net relative yaw can be calculated based on individual beam altitude as calculated angel and image material correspond. However, there are limitations for calculating the net relative yaw. Similar to the net relative distance, the yaw is dependent on an undisturbed DVL signal, i.e. fish within the vicinity is again prohibiting proper functionality. This can be observed at Fig. 13 marker f), when fish occur in the DVL vicinity. This shows that the DVL has similar

challenges as other vision based methods for estimation of net relative attitude (Duda et al. 2015 and Potyagaylo et al. 2015). Another limitation for the DVL system is that hydroacoustic beams need to be reflected back to the vehicle from both starboard and port side. Assuming a plane net and taking the 60° beam orientation in account, measurement of α is limited to the range of ± 60°. This is the explanation why there is no proper signal in Fig. 13 around marker c). Nevertheless an auto pilot yaw function keeping the ROV faced towards the net is required to operate proper around α = 0°.

The potential for using a DVL system as dead reckoning system was demonstrated in D3. Net relative velocity was measured obtained with a high sampling frequency and comparable low noise levels data. The position on the vertical net plane was obtained by numerical integration of the vertical and horizontal velocity components. The steered rectangular ROV path along the net rope structure can be reconstructed by plotting both these position components in one plane (Fig. 14 C). The accuracy of the DVL system based dead reckoning is difficult to determine, as the vehicle was manually operated. Consequently, movements were generally not straight lines and the ROVs net relative yaw was subject to additional swinging. However, the deviation in navigation data for the start-stop-point, a crossing of net ropes, is smaller than 2 m in position after traveling a distance of 60 m and a time of 9 min.
USBL and DVL depth data gathered while moving along the net pen show a systematic deviation from each other. As the starting value for the DVL system dead reckoning is set to the USBL start depth they are similar at the start of the rectangle. However as the ROV has moved down the deviation increased. When the vehicle is back at the upper edge of the rectangle pathway (Fig. 15, 180 s and 330 s), this deviation of the DVL and USBL systems depth-signal is comparably small again. As this systematic error is depth and not time-dependent, this might be based on a wrong velocity estimate of the DVL system.

As DVL data is sampled with a high frequency (5 Hz), the data from D1-3 indicate that navigational systems or auto pilot ROV-functions, i.e. constant net-distance, net-yaw and velocity controllers, can be based on it. However, results also show that the DVL signal is disturbed by fish in the vicinity of the beams (Fig. 11, Fig. 12). In the observed cases, fish occurred between net and ROV when the distances is bigger than 3 m. At these distances net integrity is nevertheless difficult to observe based

solely on visual information. For this reason, ROVs often operate closer to the net. For optimal visual performance during net inspection, no fish should be present between net and ROV.

## Conclusion

A USBL system is capable of measuring the transceiver relative position of an underwater vehicle in a commercially stocked salmon aquaculture pen with acceptable positioning precision and updating rates. The DVL system with acoustic beams projected onto a net pen produced reliable information of the net relative distance, net relative angle and velocity. However the signals from both instruments suffer from the acoustic interaction with the biomass. This becomes most prevalent when the USBL transceiver and transponder are on different sides of the net pen, or fish occur between the DVL system and net.

ROVs operating in aquaculture net pens, like for example during net inspection, can utilize standard equipment from underwater vehicles to gather navigation data. Data from a USBL system and a forward looking DVL system can support operators and quantify the achieved net inspection coverage.

Our findings suggest that the two tested instruments have the capability to support an advanced navigation system for aquaculture purposes. Further work is required that should focus on the understanding of accuracy and error issues of the individual instruments. In consequence should, even though the DVL system has not shown any tendency to lock on to structural elements behind the net, this potential navigation risk be systematically investigated. Also relevant for further work is the incorporation of the DVL and USBL systems into a multisensory fusion system, together with standard ROV sensor like compass, rate gyro and depth sensor which will provide an opportunity for an advanced navigation system. In such a system, the combination of USBL and DVL data can be utilized for estimating traveled path, net pen coverage and the given net shape. Furthermore, such a navigation system will be a fundamental requirement for full autonomous tracking of the net pen.

## Acknowledgments

The experiments are part of a project funded by the Norwegian Research Council (MerdROV/ 217541). The authors thank the project owner Lerow AS for providing the

ROV, surface vessel and crew. Thanks also to the project partner Argus Remote Systems AS and Salmar Farming AS for support and infrastructure during the trials.

**References**

K. G. Foote. Importance of the swimbladder in acoustic scattering by fish: A comparison of gadoid and mackerel target strengths. The Journal of the Acoustical Society of America. 67. 1980.

A. Duda, J. Schwendner, A. Stahl, P. Rundtop. Visual Pose Estimation for Autonomous Inspection of Fish Pens. In proceedings of MTS/IEEE Oceans 2015, Genova, Italy, May 18-21, 2015.

T. I. Fossen. Handbook of Marine Craft Hydrodynamics and Motion Control. ISBN: 9781119991496, John Wiley and Sons Ltd., 2011.

Ø. Jensen, T. Dempster, E. Thorstad, I. Uglem and A. Fredheim. Escapes of fishes from norwegian sea-cage aquaculture: causes, consequences and prevention. Aquaculture Enviroment Interactions, vol. 1, pages 71-83. 2010.

R. E. Kalman. A New Approach to Linear Filteringand Prediction Problems. ASME–Journal of Basic Engineering, no. 82 : 35-45. 1960.

P. Klebert, Ø. Patursson, P. C. Endresen, P. Rundtop, J. Birkevold, H. W. Rasmussen. Three-dimensional deformation of a large circular flexible sea cage in high currents: Field experiment and modeling. Ocean Engineering Volume 104, Pages 511–520, 2015.

P. Lader, T. Dempster, A. Fredheim, Ø. Jensen. Current induced net deformations in full-scale sea-cages for Atlantic salmon (Salmo salar). Aquaculture Engineering vol. 38, pages 52-65, 2008.

T. A. Mooney, P.E. Nachtigall, W. W. L. Au. Target Strength of a Nylon Monofilament and an Acoustically Enhanced Gillnet: Predictions of Biosonar Detection Ranges. Aquatic Mammals 30, pages 220-226. 2004.

L. Paull, S. Saeedi, M. Seto, H. Li. AUV Navigation and Localization: A Review. IEEE Journal of oceanic engineering, vol. 39, pages 131-149. 2014.

S. Potyagaylo, C. C. Constantinou, G. Georgiades. S. G. Loizou. Asynchronous UKF-based localization of an underwater robotic vehicle for aquaculture inspection operations. In proceedings of MTS/IEEE Oceans 2015, Washinghton DC, USA, October 19-22, 2015.

D. Rudolph and T. A. Wilson. Doppler Velocity Log Theory and Preliminary

Considerations for Design and Construction. In proceedings of Southeastcon 2012 conference, pages 1-7, 2012.

SNAME. Nomenclature for Treating the Motion of A Submerged Body Through a Fluid. Society of Naval Architects and Marine Engineers. Technical and Research Bulletin, no. 1-5. 1950.

Sonardyne. User Manual for Scout USBL System. Technical document, Sonardyne, UM-8068-008, Issue A-REV3. 2007.

K. Vickery. Acoustic Positioning Systems A practical Overview Of Current Systems. In Proceedings of the 1998 Workshop on Autonomous Underwater Vehicles, pages 5-17, 1998.

*Table 1: Notation for motion of a marine vehicle as set by (SNAME, 1950)*

| DOF | Name | Description | Position | Velocity |
|---|---|---|---|---|
| 1 | Surge | Motion in x-direction | x | u |
| 2 | Sway | Motion in y-direction | y | v |
| 3 | Heave | Motion in z-direction (vertical) | z | w |
| 4 | Roll | Rotation around the x-axis | φ | p |
| 5 | Pitch | Rotation around the y-axis | θ | q |
| 6 | Yaw | Rotation around the z-axis | ψ | r |

*Table 2: Notation for DVL net relative position based on the BODY reference frame*

| Name | Description | |
|---|---|---|
| Net relative distance | Slant range distance between vehicle and net along x-axis | d |
| Net relative yaw angle | Horizontal angle between vehicle and net | α |

*Table 3: DVL system parameters with settings deviating from the default*

| Description | Value |
|---|---|
| Vertical depth resolution | 1% |
| Maximum Tracking Depth | 8 m |
| Salinity | 20 |
| Coordinate Transformation | Instrument frame (BODY) |
| Adjusts the transmit pulse length to percentage of depth | 30% |
| Minimum time between pings | 0.2 s |


*Fig. 1: Argus Mariner ROV used in the experiments, here lifted over the deck of the supplying aquaculture service vessel, which was moored to the net pen floating collar (Photo: Per Rundtop)*

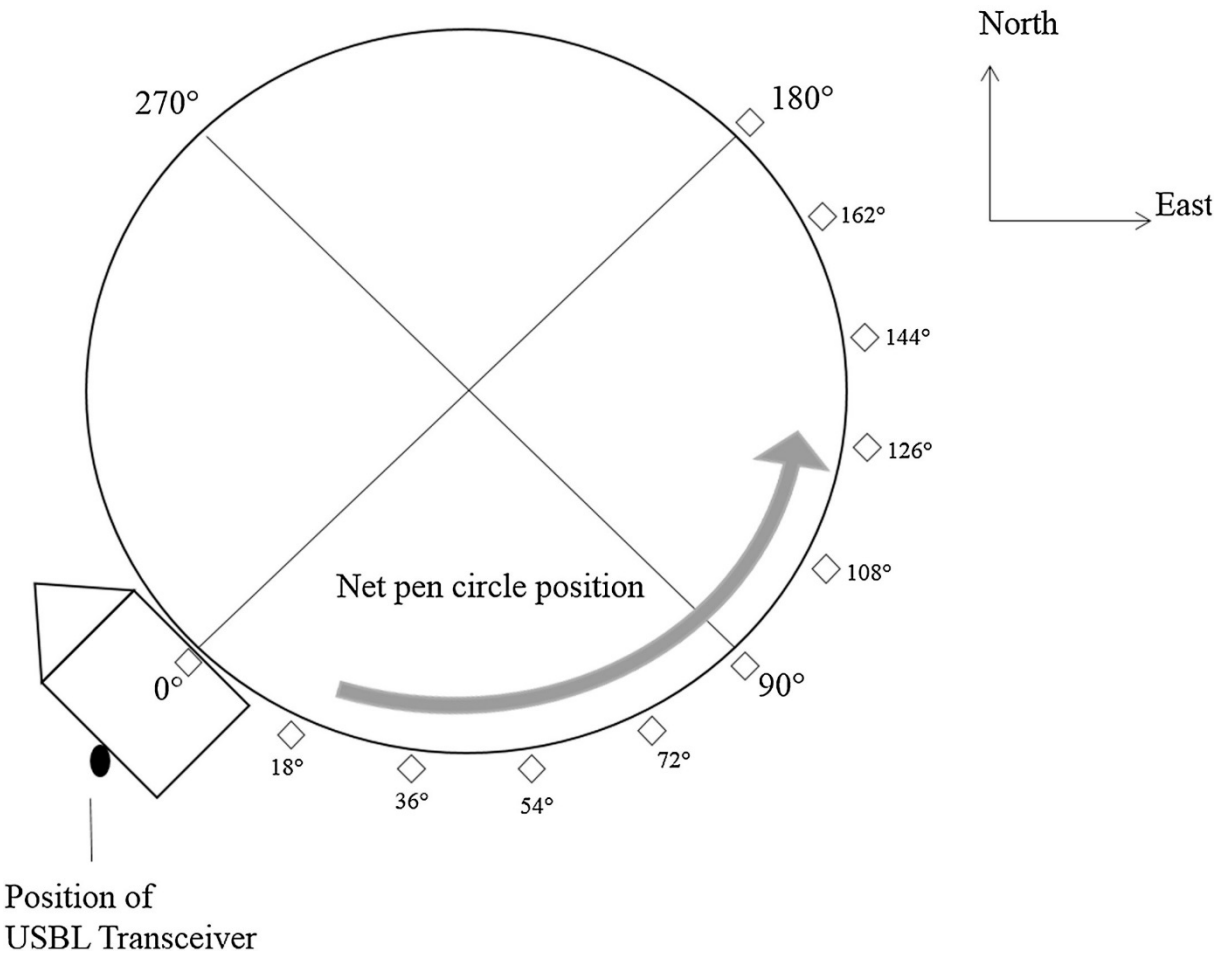


*Fig. 2: Top view illustration of the "net pen circle position" definition in degree, originating at the moored surface vessel and increasing anti-clockwise along the floating collar. Also indicated, the north-east orientation of the experimental setup, the USBL transceiver position and the USBL transponder positions for experiment U2.*

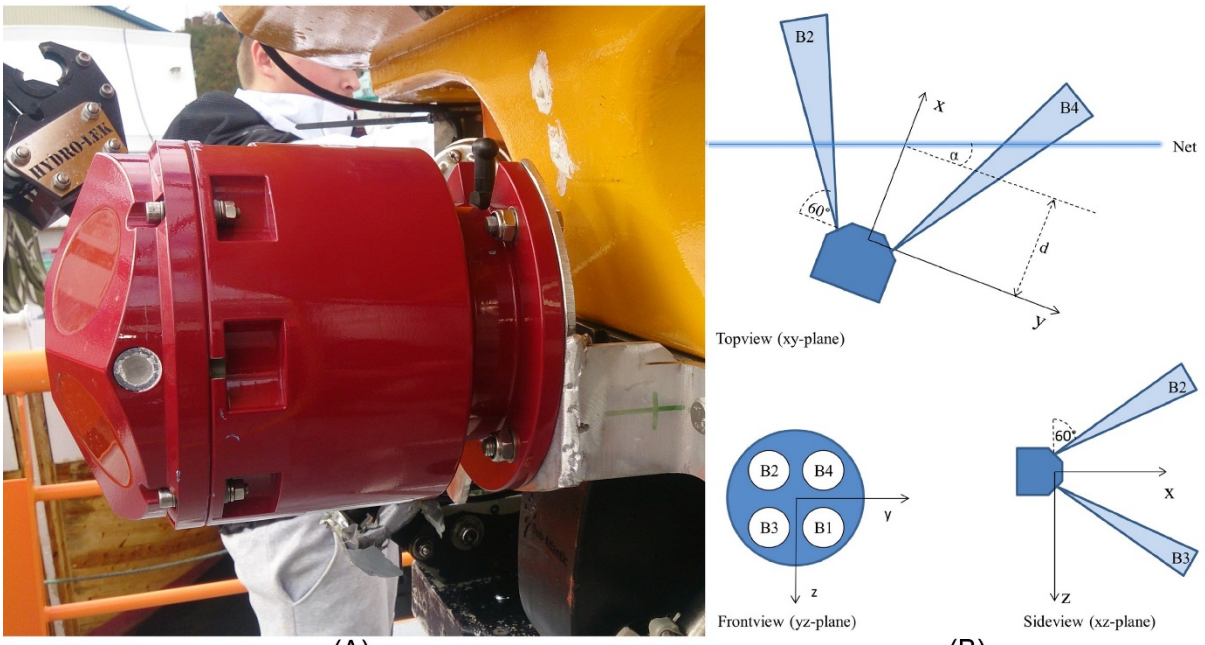


*Fig. 1: (A) DVL mounted at the front side of an Argus Mariner ROV by using a custom-made aluminum bracket (Photo: Per Rundtop). (B) Net relative yaw angle and distance of the ROV, axis in the body reference frame and beam-array orientation.*

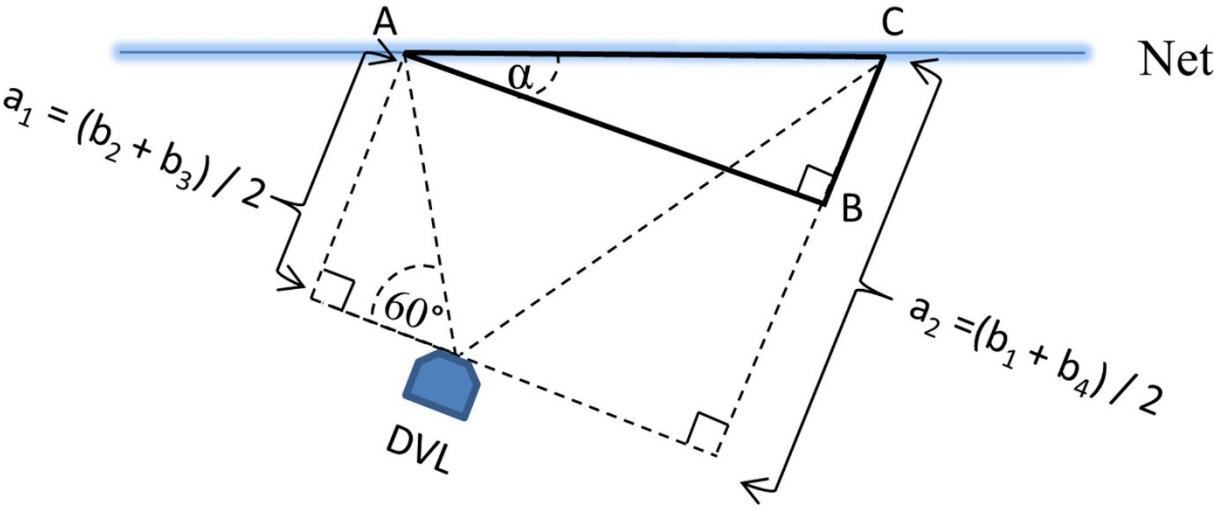


*Fig. 4: Illustration of method for calculation of the net relative yaw angle α. The calculations are based on the DVL altitudes $b_1$, $b_2$, $b_3$, $b_4$ and the known DVL beam angle of 60°.*

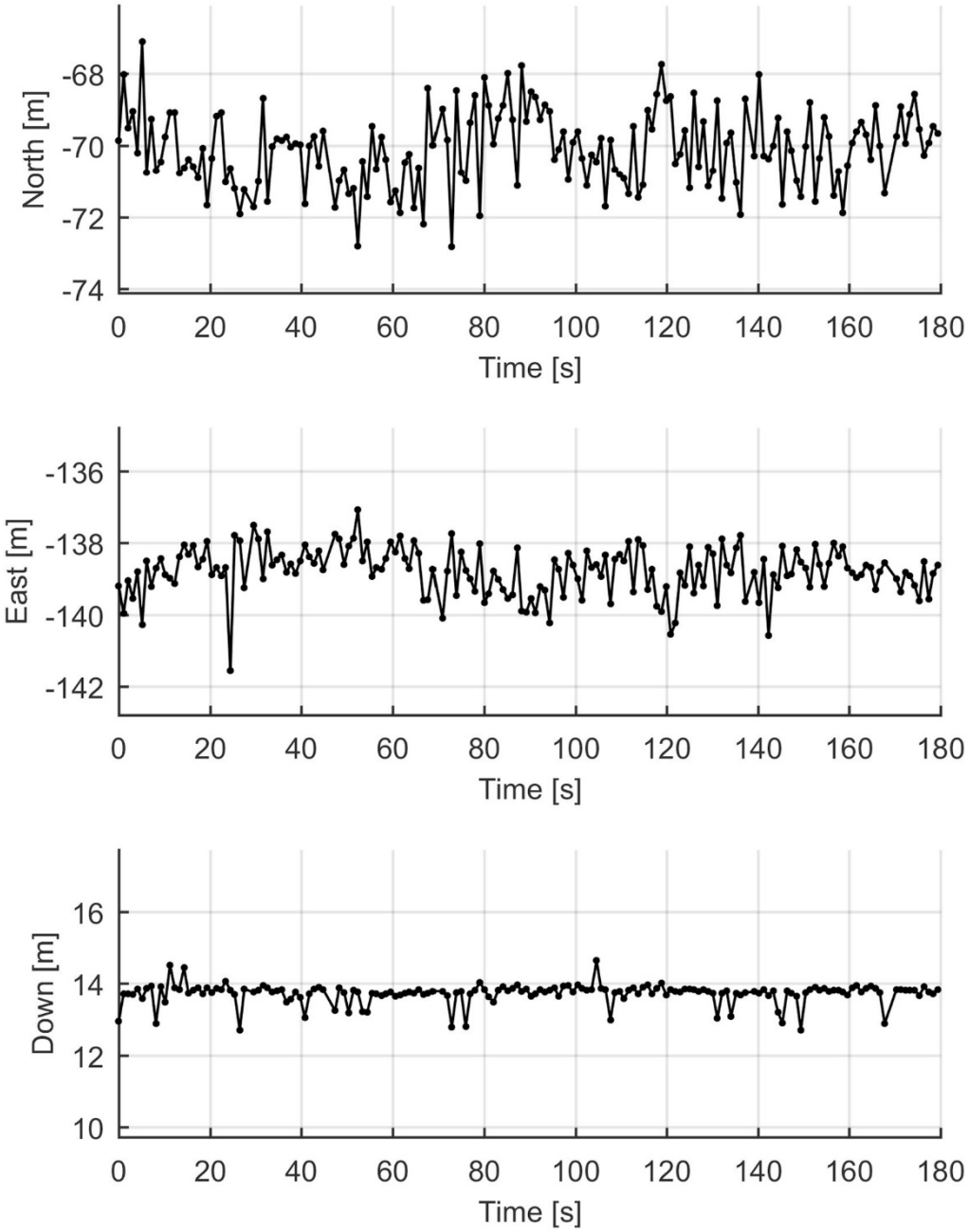


*Fig. 5: NED position time series without outliers for experiment U1*

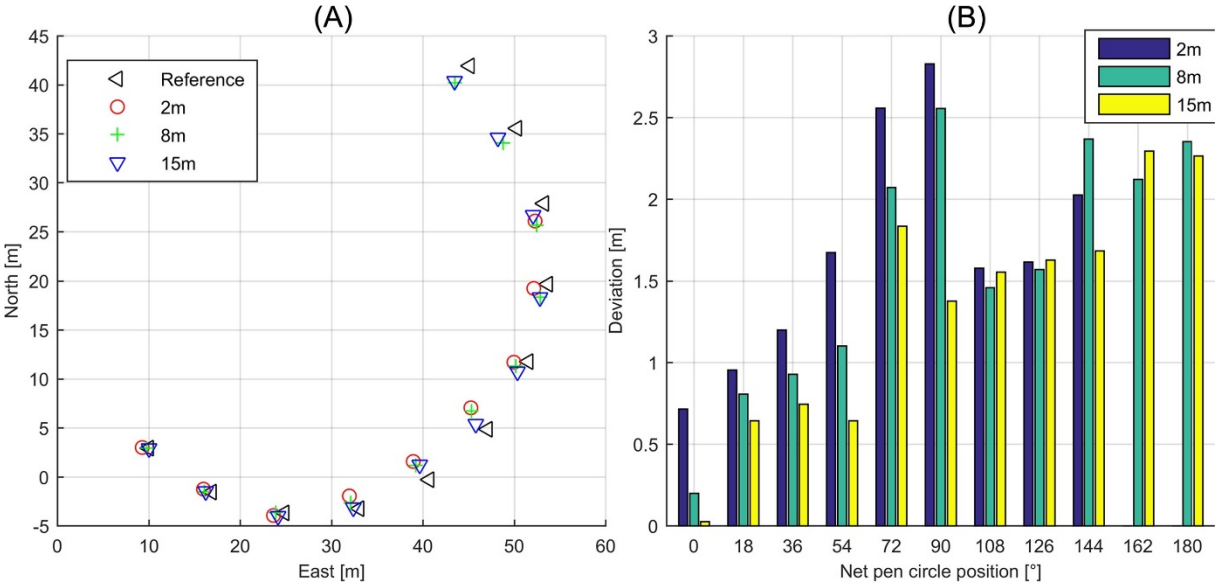


*Fig. 6: (A) Average (3 min) horizontal USBL positions with respect to a perfect circular floating collar (reference) in 3 different depths. (B) Horizontal deviation of the reference system and averaged USBL positions in the horizontal plane.*

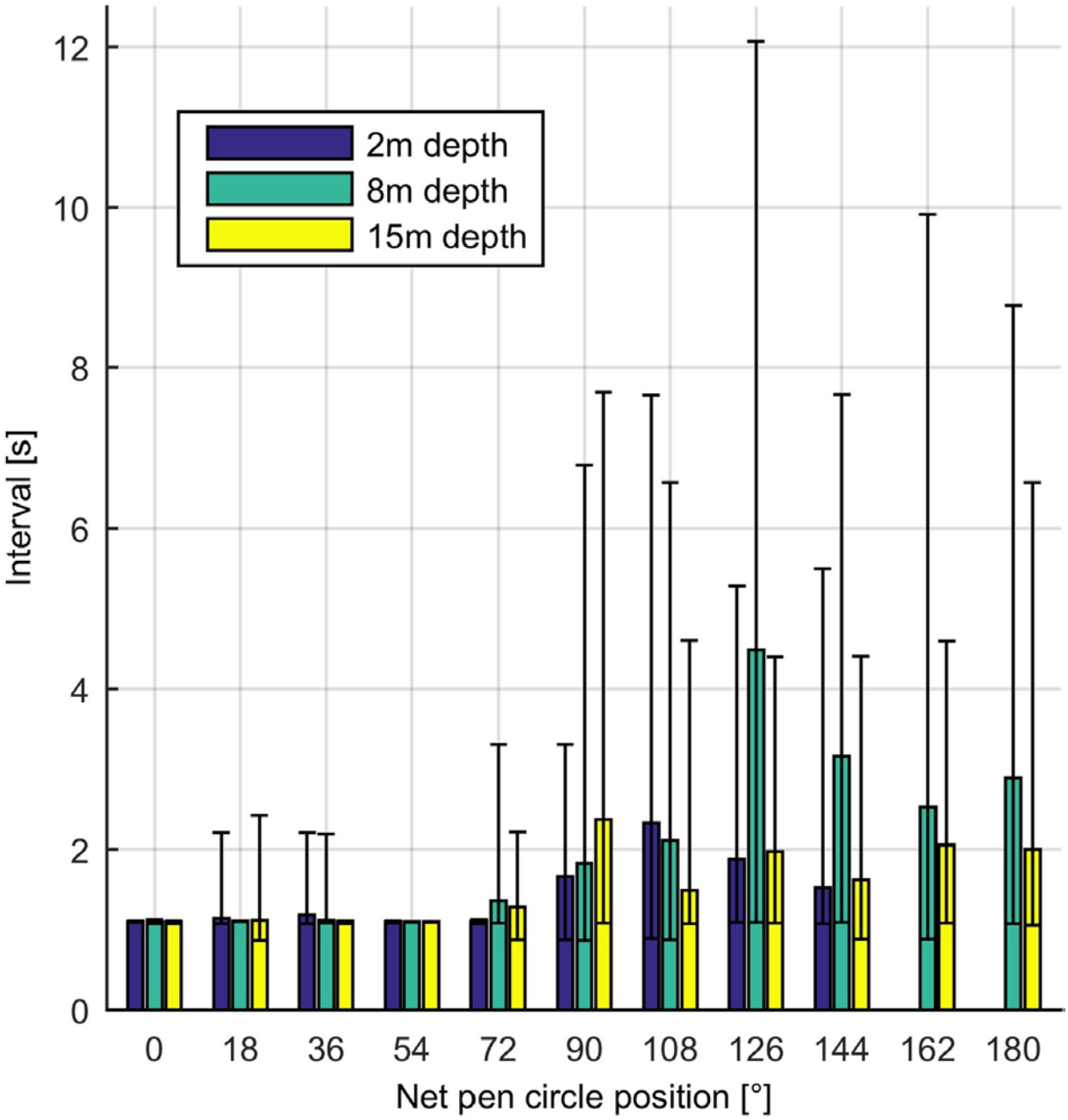


*Fig. 7: Average update intervals for USBL positions in 2 m, 8 m and 15 m depth at different net pen circle positions along the floating collar logged in the U2 experiment. Error bars indicate maximum and minimum values.*

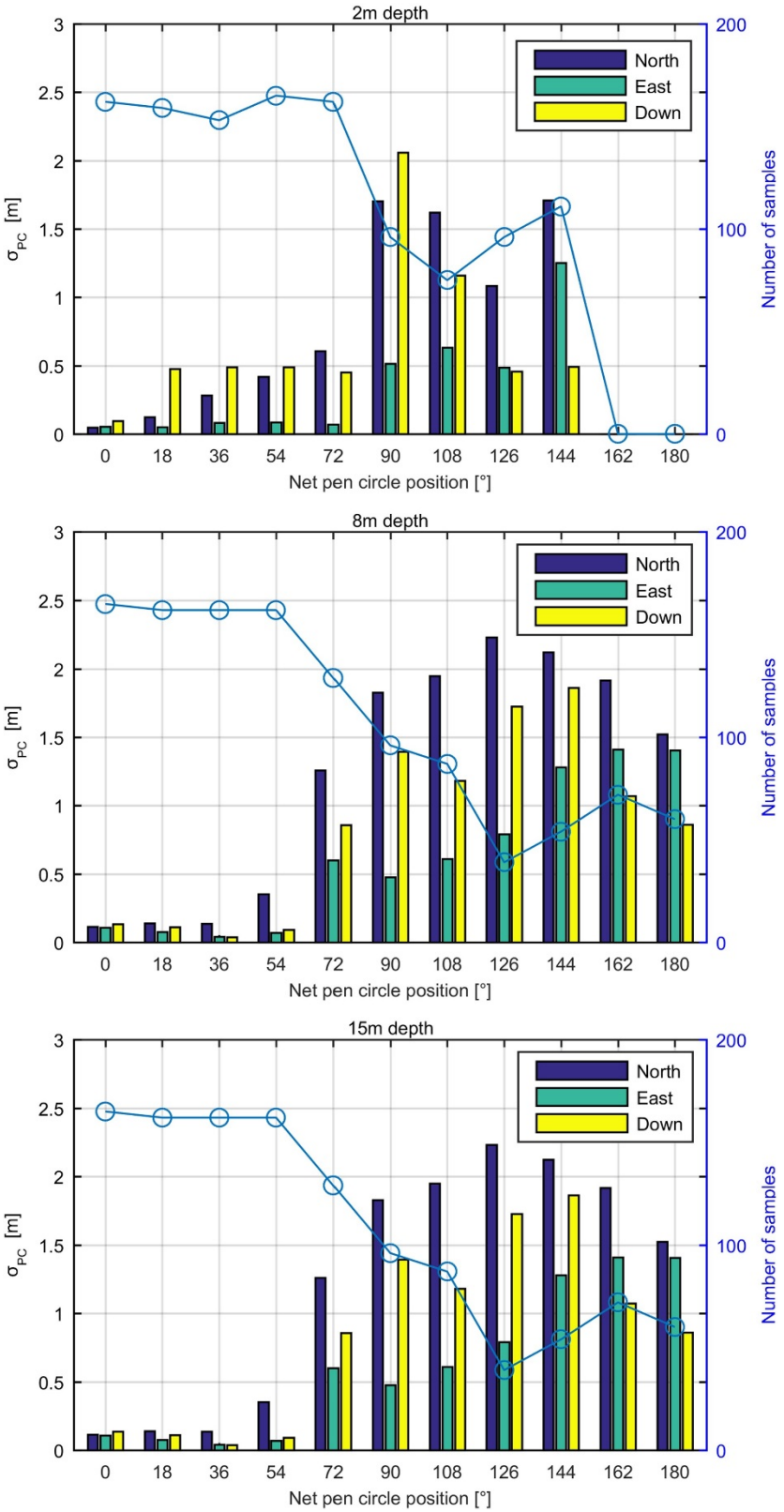


*Fig. 8: Standard deviations ($\sigma_{PC}$) and obtained numbers of samples on the north-, east- and depth-axis for USBL positions at different net pen circle positions and in depths of 2 m, 8 m and 15 m and.*

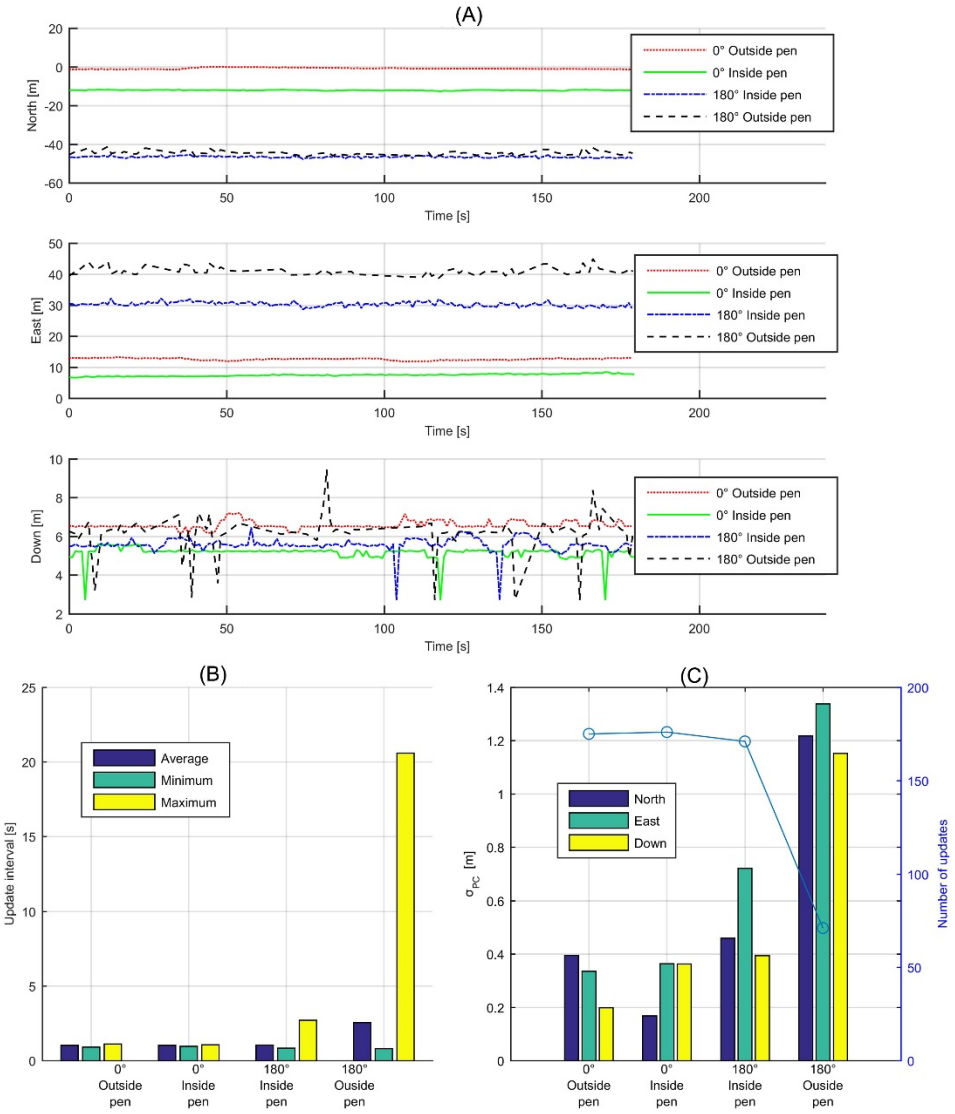


*Fig. 9: (A) time series for U3 in NED and (B) Update intervals and (C) $\sigma_{PC}$ from 3 min periods at USBL positions in 5 m depth, at 0° and 180° net pen circle positions as well as inside and outside the net pen.*

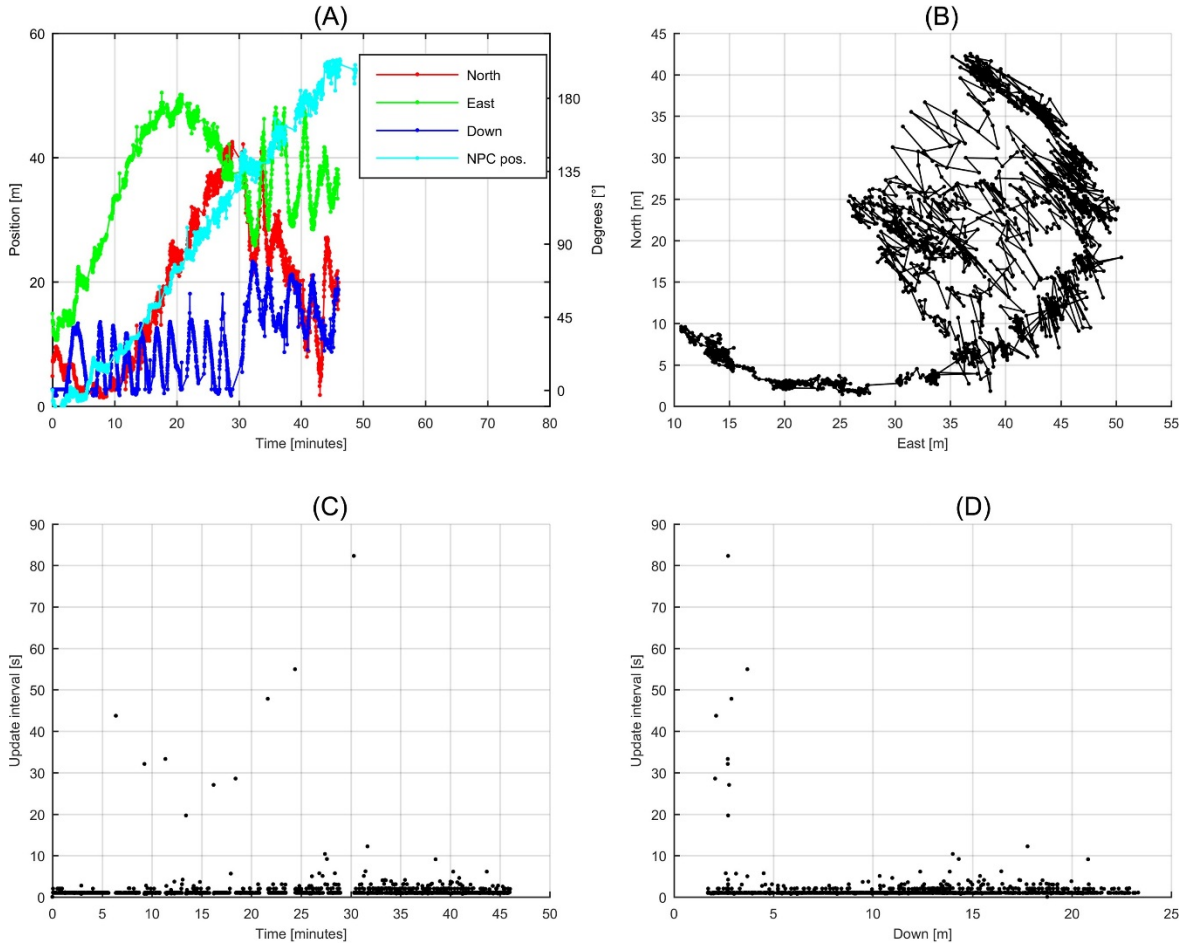


*Fig. 10: (A) Time series for the estimated net pen circle position and ROV position coordinates in north, east and down during inspection of half of the circular net pen wall (0 – 30 min) and approximately1/3 of the conical net pen bottom (30 - 45 min). (B) USBL positions in the horizontal plane. (C) Position update interval plotted as a function of time. (D) Position update interval plotted as a function of the vehicles depth.*

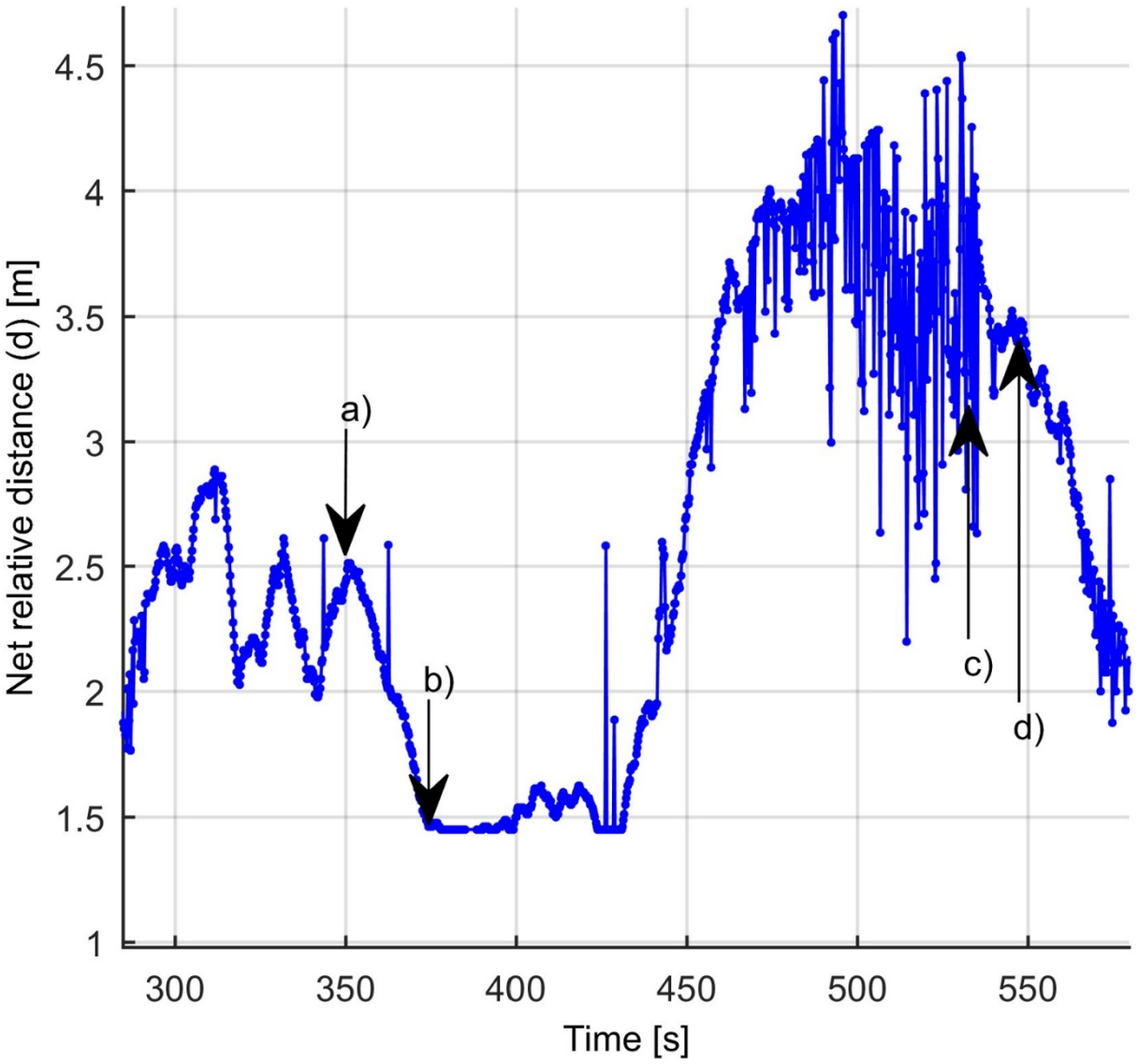


*Fig. 11: Example of the net relative distance determined by the DVL system while moving the ROV away from and towards the net in the range of 1.5 - 4 m. Letters indicate the corresponding time for the pictures shown in Fig. 12. The net relative distances at a), b), c) and d) is expected to be comparable, the rapid changes in distance in ca. 50 s period before c) is expected to be a consequence of fish in the vicinity of the DVL system.*

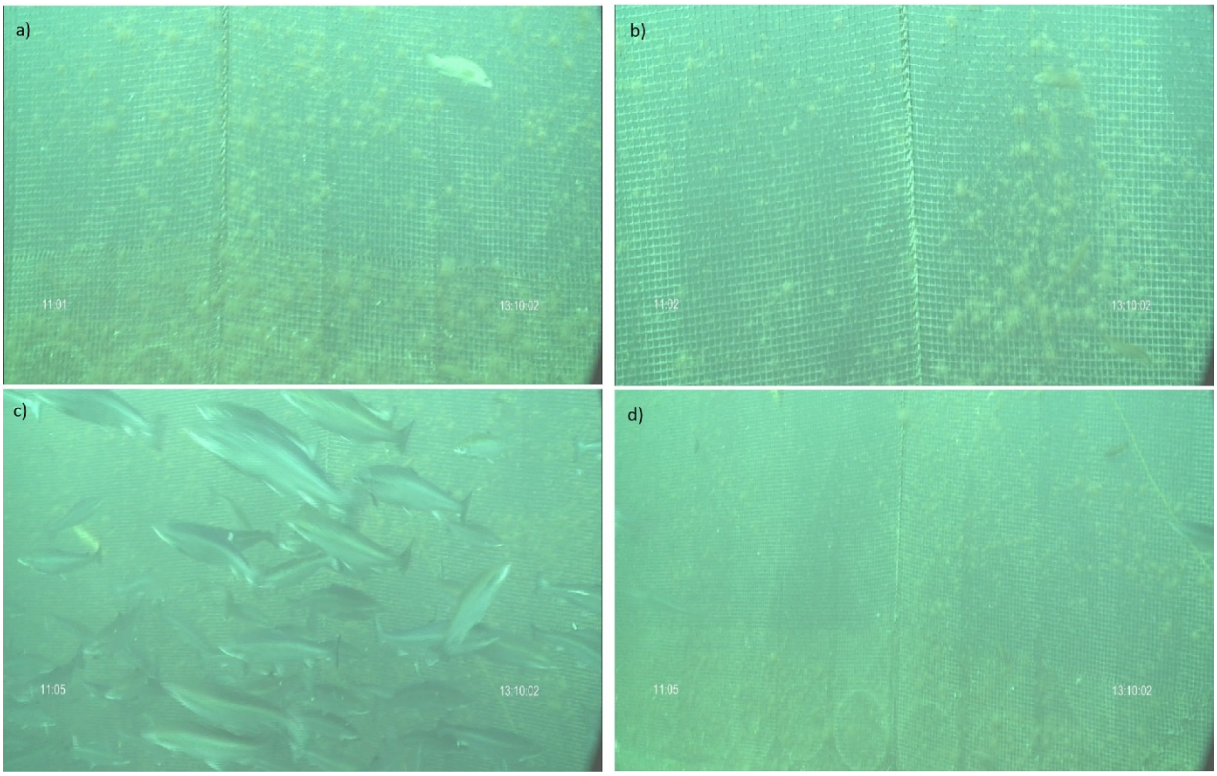


*Fig. 12: ROV camera images at different times during the testing of the DVL system ability to determine relative net distance. Net distance determined are for a) 2.5 m and b) 1.5 m; c) and d) were taken at almost the same distance expected to be 3.5 m (compare Fig. 11).*

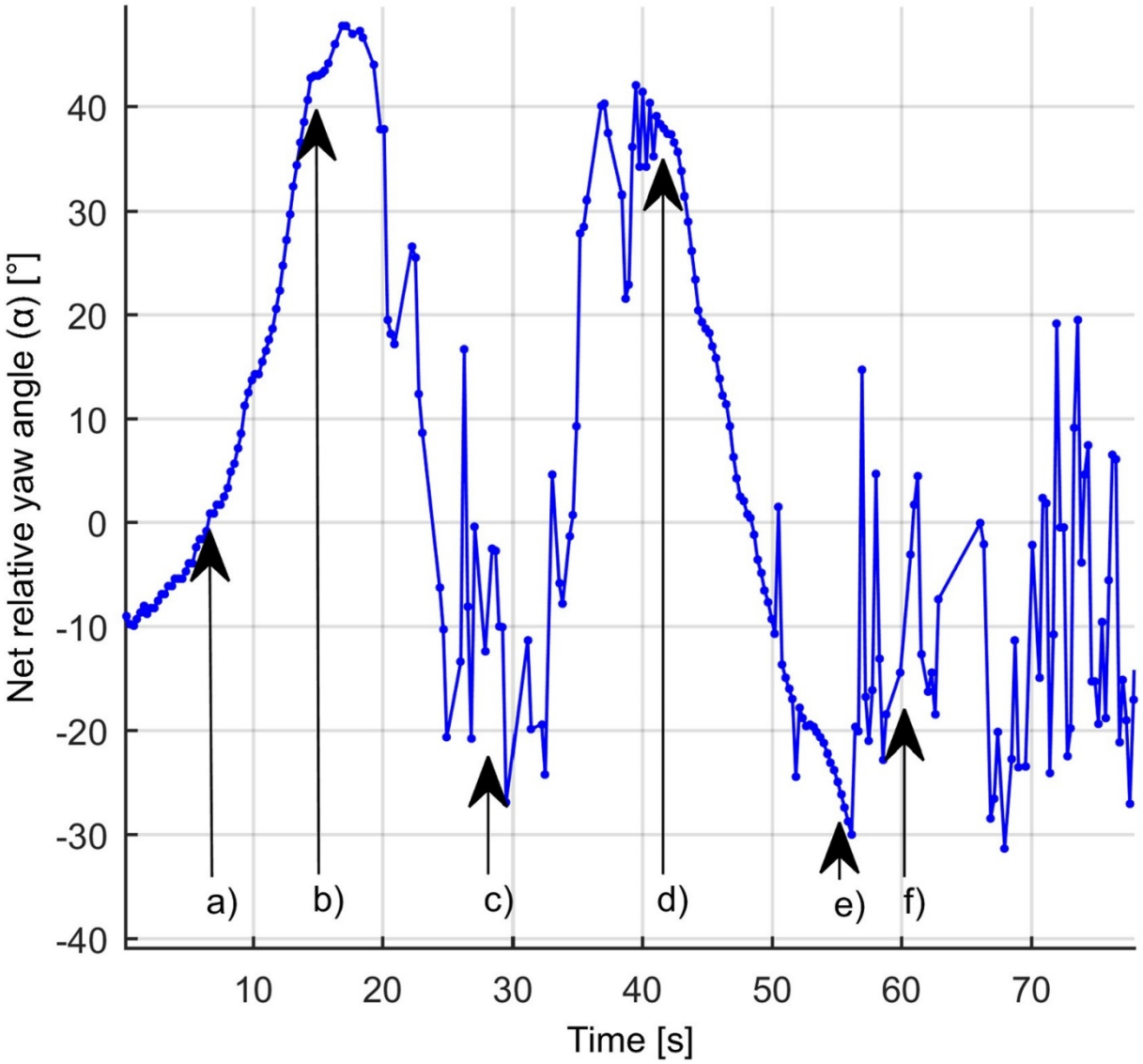


*Fig. 13: Calculated net relative yaw angles of the ROV placed approximately 4 m from the net and swinging approximately from α=0° to α=90° and back to α=-90°. The marked yaw position are estimated from camera images as a) 0°, b) 45°, c) 90°, d) 40° e) -30°, f) -40°.*

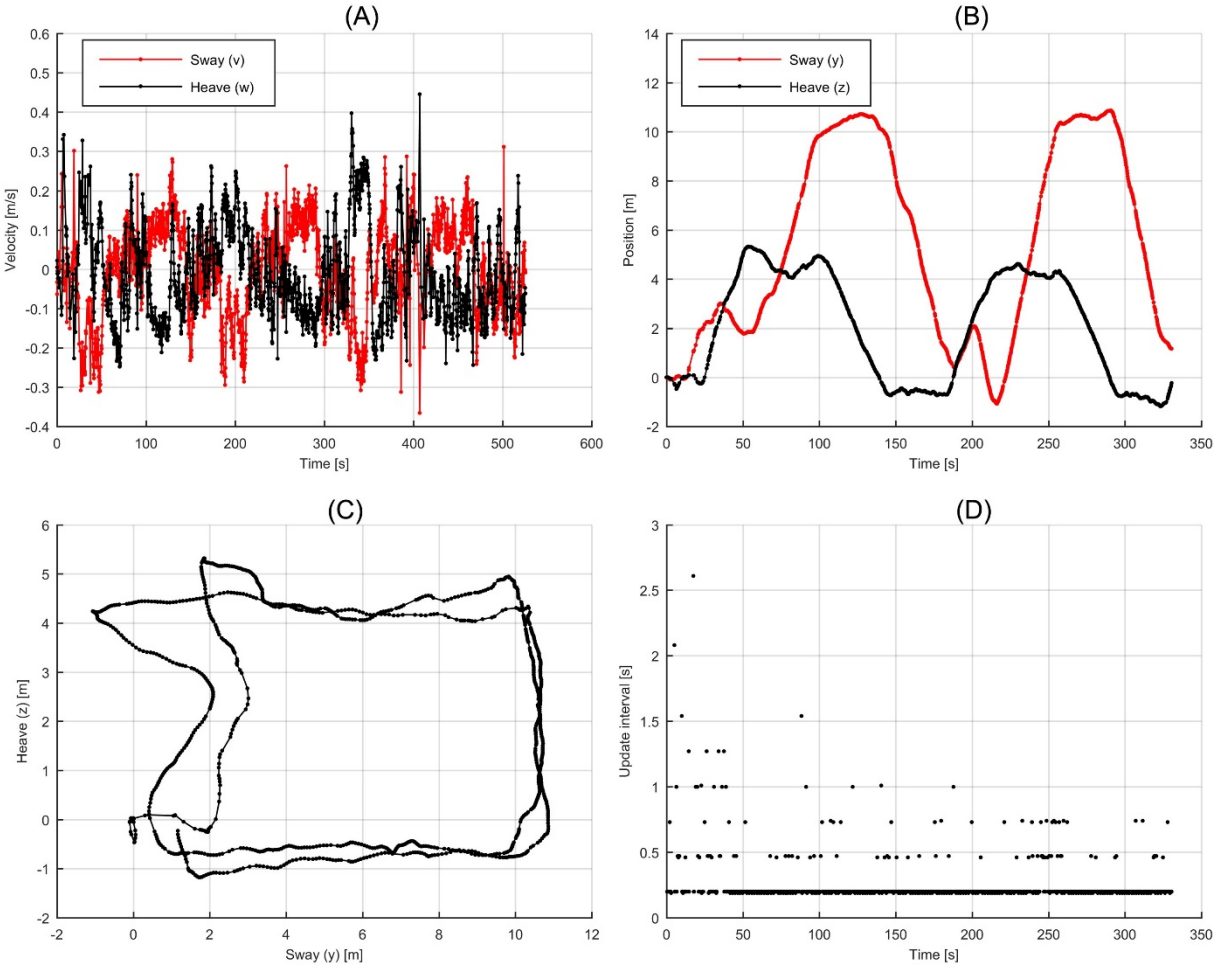


*Fig. 14: (A) ROV velocity relatively to the vertical net pen wall measured by the DVL system, with heave as vertical velocity and sway as sideways velocity component of the vehicle (BODY reference frame). (B) Integration of the two velocity components, providing depth and sideways displacement on the net pen plane. (C) Net pen plane movement pattern based on DVL signals. (D) Time series of the update interval.*

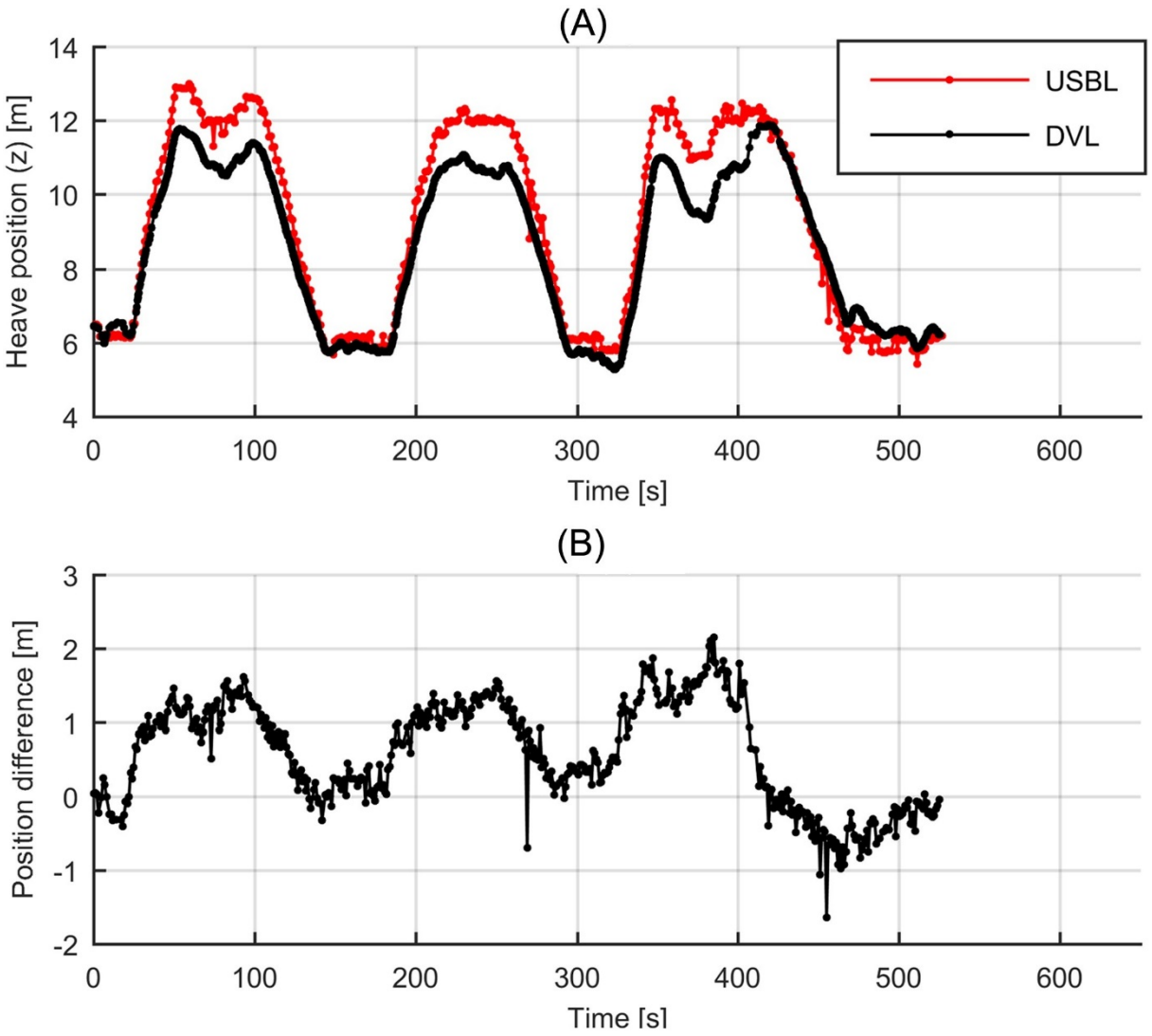


*Fig. 15: (A) Time series on heave position obtained from the USBL system and dead reckoning calculated from DVL data. (B) The difference in heave position between USBL and DVL. DVL system dead reckoning position for t=0 is set equal USBL system depth t=0.*